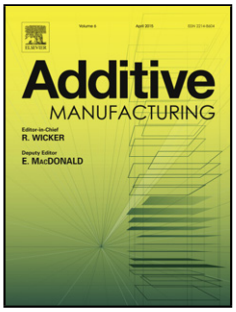

Title: Additive manufacturing of heat-sensitive polymer melt using a pellet-fed material extrusion

Authors: Zuoxin Zhou, Iulia Salaoru, Peter Morris, Gregory J. Gibbons

PII: S2214-8604(18)30368-3
DOI: https://doi.org/10.1016/j.addma.2018.10.040
Reference: ADDMA 564

To appear in:

Received date: 29-5-2018
Revised date: 14-9-2018
Accepted date: 23-10-2018

Please cite this article as: Zhou Z, Salaoru I, Morris P, Gibbons GJ, Additive manufacturing of heat-sensitive polymer melt using a pellet-fed material extrusion, *Additive Manufacturing* (2018), https://doi.org/10.1016/j.addma.2018.10.040

Additive Manufacturing of Heat-Sensitive Polymer Melt using a Pellet-Fed Material Extrusion

Zuoxin Zhou [1, 2], Iulia Salaoru [1, 3], Peter Morris [4], and Gregory J. Gibbons [1, *]

1. WMG, the University of Warwick, Coventry, UK
2. Centre for Additive Manufacturing, Faculty of Engineering, the University of Nottingham, Nottingham, UK
3. EMTERC, De Montfort University, The Gateway, Leicester, UK
4. PVOH Polymer Ltd., Global Business Park, Wilkinson Road, Cirencester, UK

*Corresponding Author: Tel: +44 (0)24 7652 2524
Email: G.J.Gibbons@warwick.ac.uk (Dr. G. Gibbons)
Postal Address: WMG, International Manufacturing Centre, University of Warwick,
Coventry, UK, CV4 7AL

Abstract

The most common method for Additive Manufacturing (AM) of polymers is melt extrusion, which normally requires several pre-processing steps to compound and extrude filament feedstock, resulting in an overall long melt residency time. Consequently a typical melt extrusion-based AM process is time/cost consuming, and limited in the availability of materials that can be processed. Polyvinyl alcohol (PVOH) is one of the heat-sensitive polymers demonstrating a thermal decomposition temperature overlapping its processing window. This study proposed to use a pellet-fed material extrusion technique to directly process PVOH granules without the necessity of using any pre-processing steps. The approach essentially combined compounding, extrusion and AM, allowing multi-material printing with minimum exposure to heat during the process. The processing parameters were determined via thermal and rheological characterisation of PVOH. Effects of processing temperature and time on the thermal decomposition of PVOH were demonstrated, which further affected the tensile properties and solubility. An increase in Young’s modulus, stress at 2% strain, and Ultimate Tensile Stress were 98±4%, 40±5%, and 20±2%, respectively, was observed when PVOH residency time was reduced from 25min to 14min. The pellet-fed material extrusion technology demonstrated good 3D printability, multi-material printing capability, and great versatility in processing polymer melts.

Keywords

Additive Manufacturing, Three-Dimensional Printing, polyvinyl alcohol, thermal decomposition, material extrusion

1. Introduction

Polyvinyl alcohol (PVOH) is a linear synthetic polymer prepared by partial or full hydrolysis of polyvinyl acetate (PVA), polymerised from vinyl acetate. Partial hydrolysis essentially results in a copolymer of PVOH and PVA (**Figure 1**). The small amount of residual acetate groups weaken the inter- and intra-molecular hydrogen bonding of adjacent hydroxyl groups, thus allowing the material to be dissolved in water [1]. Due to its water solubility, non-toxicity, and biodegradability, PVOH has been used for a wide range of applications, including food packaging, medical devices, drug delivery, paper coating and consumer goods [2-5]. However, it is often processed using solvent casting instead of a more versatile and economically favoured melt-processing method due to a concern over its thermal decomposition [6, 7]. The thermal decomposition of PVOH starts with the elimination of hydroxyl groups at a temperature close to the melting point (T_m), which is between 180-240 °C, depending on the hydrolysis level, degree of crystallinity, and additives in the compound [6, 8]. The elimination of the hydroxyl pendant group is also time-dependent. A 33 wt% loss for PVOH was reported after a four-day isothermal experiment at 195 °C [9]. Therefore, a short residency time, and ideally minimum manufacturing steps, are necessary to melt process PVOH.

Recently, partially hydrolysed PVOH has also been used as a water-soluble support material or a binding additive to facilitate Additive Manufacturing (AM) processes. AM or Three-Dimensional Printing (3DP) includes a series of manufacturing technologies to build 3D objects from a computer-aided design (CAD) model via layer-by-layer fabrication. PVOH was used as an efficient additive to bind with aqueous liquid and subsequently provided sufficient binding strength to bioceramic powders [10-12]. It was also used as a removable mould for indirect material extrusion fabrication [13]. Direct AM fabrication using PVOH has focused on controlled delivery of actives for pharmaceutical and laundry applications using either piezoelectric inkjet printing [14, 15] or material extrusion [16-17]. Due to the restriction in ink viscosity, piezoelectric inkjet printing is usually used in printing multilayer film structures with a thickness in the micrometre range [14]. Material extrusion can be used to build a 3D part via extruding a thermoplastic-based filament through a hot printhead and subsequently depositing the melt in layer-by-layer. Studies have attempted to control the thermal decomposition of PVOH by using a lower liquefier temperature or incorporating lubricants to decrease the melt temperature (T_m) [18, 19]. Nevertheless, the material is subjected to a three-step melt process including 1) mixing of different compounds, 2) extruding filament feedstock and 3) material extrusion. This extended processing results in a long residency time and excessive thermal decomposition of PVOH.

To address this issue, a pellet-fed material extrusion system has been developed and used combining AM with a conventional single-screw extrusion [20]. Pellet materials can be processed directly using this technology. Therefore, the residual time of polymer melt is significantly reduced as pre-processes to compound and extrude filament are not required. It is an ideal technology to process heat-sensitive polymers or materials that are difficult to extrude into filament with a consistent diameter. Additionally, this technology allows co-processing of multiple materials at different and variable rates fed into the extruder to fabricate a compositionally heterogeneous structure. Commercially available pellet-fed material extrusion systems include 3DDiscovery^{TM} (regenHU, Switzerland) – focused on biomaterials, Gigabot X (re:3D Inc., US), ATLAS^{TM} (Titan Robotics, US) and BAAM (Cincinnati, US). However, these have emerged onto the market within the time-frame of this research. The vast majority of material extrusion system are still using filament feedstock.

The aim of this study is to propose an AM technology that is more appropriate for processing heat-sensitive material, in particular PVOH. Four objectives are involved in this study in order to reach the aim, including (1) designing and constructing a pellet-fed material extrusion that is capable of tuning the processing residency time; (2) determining the processing conditions for PVOH via material characterisations using thermal and rheological testing; (3) demonstrating 3D printing capability including dimensional accuracy, interface coalescence, and compound mixing; and (4) characterising the effects of residency time on the performance of PVOH structures.

2. Methodology

2.1. Design and Construction of the Direct-Feed Material Extrusion

A preliminary study has developed a vertical single-screw extruder with a size that can fit inside a typical desktop material extrusion AM machine (shown schematically in **Figure 2**) [20]. It has four feeding ports at different heights along the barrel to provide a wide range of residency times. Two heaters are located inside the barrel to raise the processing temperature. Polymer melt is sheared by the screw, conveyed through the nozzle into a hot printhead, and eventually deposited onto a substrate or previously printed structure. Screw rotational speed is controlled by the stepper motor, which determines the depositional speed of the material. The extruder is integrated with a commercial 3D printing platform (Touch 3D, Cubify, US) to enable controlled 3D movement and controlled deposition to generate 3D objects according to the CAD design.

The Touch 3D platform was modified to replace the printing unit with the new extruder to enable pellet-fed material extrusion (**Figure 3**). The printbed integrated into the equipment was capable of heating up to 110°C to allow better adhesion of the first layer of material. A temperature controller receives an input from a thermocouple located close to the nozzle, and an output to cartridge heaters. Ceramic insulating plates were used to reduce thermal radiation and conduction to heat-sensitive components, such as the stepper motor and bearings, by creating gaps between them and the heated barrel. A titanium screw was manufactured using laser-Powder Bed Fusion (EOS M270, EOS GmbH, Germany) with the following configuration: shaft diameter = 12 mm, shaft length = 206.24 mm, flight depth = 1.5 mm, flight thickness = 1 mm, and flight distance = 14.93 mm. A small flight depth and a large flight distance was designed to (1) minimise the amount of materials required to fill the free space in the barrel; and also to (2) avoid extensive heat generated during the process due to shearing. In this study, PVOH was fed into the extruder using the lowest port to reduce thermal residence time. The effective area on the screw was polished using SiC paper to minimise material adhesion to the screw during melt processing.

2.2. Thermal and Rheological Characterisation

Thermal and rheological properties of a commercial PVOH compound used in this study were characterised to determine the extruder and liquefier temperatures. The compound was based on a partially hydrolysed PVOH grade with a hydrolysis level of 86.5-89.0%. The number average molecular weight (M_n) of PVOH was 23,810 and the polydispersity was 1.75, determined by gel permeation chromatography (GPC). The PVOH compound was in powder form. Differential Scanning Calorimetry (DSC) analysis of PVOH was made using a DSC1 Star System (Mettler Toledo, Switzerland) under flowing N_2. A sample of approximately 6 mg was sealed in an aluminium pan and heated from 25 °C to 225 °C at a heating rate of 10 °C/min. The DSC measurements were repeated three times.

Thermo-Gravimetric Analysis (TGA) was carried out using Mettler Toledo TGA1-STARe (Mettler Toledo, Switzerland). Each PVOH sample of approximately 10 mg was loaded in an aluminium pan and heated from 25 °C to 450 °C at a heating rate of 10 °C/min under flowing N_2. The onset thermal decomposition temperature was determined from the mass loss curve. Samples were also tested under isothermal conditions for 15 min heating at 200, 225, and 250 °C in order to assess the effect of time on the thermal decomposition of PVOH at various temperatures, and providing insight into residency-related thermal decomposition.

Oscillatory melt rheology was carried out using a Thermo-Haake MARS III rotational rheometer (Thermo Fisher Scientific, United State). Measurements were performed in an oscillatory shear mode using a parallel plate geometer (15 mm ϕ) with 1 mm gap. Frequency sweeps from 0.1 Hz to 100 Hz were carried out at temperatures ranging from 180 °C to 210 °C. Shear stress was set at 2 Pa, predetermined from the linear viscoelastic limit of the material under test.

2.3. Additive Manufacturing and Characterisation

A complex 3D structure was designed to combine a variety of feature types including walls, holes, incremented stairs, and spherical surfaces, and similar to a structure used in a benchmark report [21]. The structure was manufactured from PVOH using the pellet-fed material extrusion system. Based on the thermal and rheological results, the extrusion and liquefier temperatures were set at 178 °C and 200 °C, respectively. Extrusion motor speed (70 rpm) was determined after preliminary trial runs to ensure that the deposition speed coincided with the head movement speed to provide consistent deposited polymer tracks of

0.5 mm height (layer thickness). Printing accuracy was determined by evaluating and comparing the feature size with the CAD design.

The ability to print multi-material was demonstrated via co-feeding and subsequently printing PVOH with a fluorescent whitening agent (FWA), which can be characterised quantitatively to reveal the compositional distribution [22]. FWA was at 1wt.% and without any pre-mixing. A simple rod-shaped sample (4 mm ϕ x 20 mm height) was printed using the above-mentioned processing parameters. The printed sample was sectioned longitudinally into small samples, each of which was subsequently dissolved in deionised water at 0.63 x 10^{-2} g/ml. Each prepared sample was characterised using UV-vis (Cary 60, Agilent Technologies, US) and fluorescence spectroscopy at an excitation wavelength of 312 nm (FP-6500, Jasco, UK). The same processing and characterisation was performed on PVOH without incorporation of FWA additive.

Sample morphology was imaged using a Zeiss Sigma Field Emission Scanning Electron Microscopy (SEM) (Carl Zeiss AG, Germany), operating with a 5-10 kV accelerating voltage. The imaged structure was mounted on an aluminium stub using a cold cure resin (Extec Corp, Enfield, CT 06083-1258, US), allowed to cure for 24±2 h and subsequently gold-coated using a sputter chamber prior to SEM examination.

The effects of melt residency time on the chemical groups, tensile properties, and solubility was investigated by feeding PVOH at the two lowest ports on the extruder, resulting in two different melt residency times of 14 min and 25 min when a sample was printed at a 0.5mm layer thickness (70 rpm extruder motor speed). The melt residency time was determined based on the volume within the conveyance system from the feeding port to the liquefier nozzle, and the volumetric depositional speed.

Tensile testing of PVOH samples processed under different residency times was carried out using an Instron 4465 tensile machine (Instron, United State) with a 5kN load cell, according to ISO 527-1:1996. Five samples were tested for each residency time. Samples were printed with a total length of 75 mm, a gauge length of 25 mm, and a thickness of 2 mm and tested using a 2 mm/min crosshead speed until failure. Young's modulus was determined from the slope of the initial linear region of the stress-strain curve up to 2 % strain. Stress at 2 % strain, strain at break and ultimate tensile strength were also determined from the stress-strain curve.

Fourier-transform infrared spectroscopy (FTIR) spectra were obtained on a Perkin-Elmer Paragon 1000PC spectrometer (Perkin-Elmer, United State) using a 800-3800 cm^{-1} wavenumber range, with 4 cm^{-1} resolution and each spectrum averaged over 16 scans. The spectra of three specimens were collected for each sample pre-processed under different residency times and using the PVOH raw material as the control sample.

Rectangular samples (35mm x 20mm x 1mm) were also printed with different melt residency times and subsequently immersed in 20 ml of deionised/distilled water at room temperature (20±2 °C) with magnetic stirring applied at 3500 rpm. The times at which each specimen initially started to distort and when completely dissolved were recorded. Five specimens were tested for each residency time.

2.4. Statistical Analysis

SPSS13.0 software (SPSS, USA) was used to analyse the data. One-way Analysis of Variance (ANOVA) with post-hoc Bonferroni correction was used to calculate statistical significance between tested groups, based on normal probability tests. A p-value less than 0.05 denoted significance.

3. Results and Discussion

3.1. Processing Parameter Determination

It is well documented that at 240°C PVOH starts to eliminate acetaldehyde, unsaturated aldehydes and ketones, benzene and benzene derivatives as products of decomposition [23]. However, water is pre-released below 240°C as a result of elimination of hydroxyl pendant group, which overlaps the processing temperature of PVOH, making this material highly sensitive to thermal processing. Therefore, a comprehensive investigation of its thermal and rheological properties was carried out to determine appropriate parameters to process PVOH in the pellet-fed material extrusion system.

The PVOH used in this study was found to have a crystalline melting point, T_m, of 178±1 °C and a glass transition, T_g, of 56±1 °C (**Figure 4**). The area of the crystalline melting peak was used to deduce the degree of crystallinity based on a heat of fusion value (ΔH_f = 6.87 kJ/mol) from literature [24]. It was then calculated that the degree of crystallinity was 17±2 %. The DSC result suggested a processing temperature above 178°C was necessary to melt the PVOH.

Both non-isothermal and isothermal TGA were carried out to reveal effects of temperature and time on the thermal decomposition of PVOH. The non-isothermal TGA demonstrated a major mass loss occurring at an extrapolated onset temperature of 286 °C, which can be related to the breakdown of the polymer backbone (**Figure 5 a**). Additionally, a 7.8 % mass loss was observed prior to the major decomposition, consistent with previous studies indicating that pendant groups were eliminated at a lower temperature. Samples subjected to isothermal TGA at different temperatures demonstrated different degrees of decomposition. Following first order kinetics, samples decomposed up to 0.56 %, 1.63 %, and 7.23 %, respectively, for 15 min heat treatment at 200 °C, 225 °C, and 250 °C (**Figure 5 b**). A yellow residual was received after isothermal TGA at 250 °C, which did not occur for the other residuals, suggesting no backbone breakdown occurring at 200 °C and 225 °C. Therefore, all the mass loss found at lower temperatures was solely related to hydroxyl group elimination. Degradation was therefore found to be both temperature and time dependent. Therefore, processing PVOH using a lower temperature and short residency time would be required to minimise thermal decomposition.

An oscillatory rheological analysis was carried out to further investigate the rheological behaviour of PVOH at different temperatures. The complex viscosity decreased when the frequency or the temperature increased (**Figure 6 a**). This was due to the disentanglement and increased mobility of molecular chains at higher shear rates and temperatures. A significant decrease in the viscosity was observed at 200 °C and 210 °C. The viscoelastic behaviour of the polymer was indicated by the change in storage modulus $G^{'}$ and loss modulus $G^{''}$. Both $G^{'}$ and $G^{''}$ increased with the increase in shear frequency up to 60Hz and then $G^{''}$ decreased (**Figure 6 b**). PVOH exhibited a more liquid-like (viscous) behaviour at lower shear frequencies with $G^{''}$ higher than $G^{'}$; at higher shear frequencies it became more solid-like (elastic). Viscosity of polymers is both temperature and shear rate dependent. For a typical material extrusion process, polymer melt is subjected initially to relatively low shear rates, followed by high shear rates (100-200 s^{-1}) when extruded through the nozzle [25]. However, high shear rate should also be expected in the extrusion for the pellet-fed material extrusion process. PVOH demonstrated a shear-thinning behaviour as the complex viscosity reduced significant at high shear rate favouring the process.

Based on the thermal and rheological results, the extrusion temperature was determined to be 178 °C. This extrusion temperature will ensure PVOH being highly molten whilst without being exposed extensively to heat. Despite a relatively high melt viscosity at 178 °C, screw shearing provided by the stepper motor should be sufficient to convey PVOH melt towards the liquefier. However, a higher temperature (200 °C) was selected in the liquefier due to (1) no screw shearing force applied to this region; and (2) a high pressure drop at the nozzle. Rheology results demonstrated a significant drop in the melt viscosity at 200 °C, which would facilitate depositing PVOH out of the nozzle.

3.2. 3D Printing Capability

Following the determination of the processing temperatures, the printing speed was calibrated to correlate with the screw rotational speed so as to ensure a precise control of the material deposition. The 3D printability was demonstrated by printing out a complex structure designed to comprise different features (**Figure 7**). The printed structure accurately represented its CAD design including details such as thin walls, holes with different diameters, a ball structure and incremented steps both horizontally and vertically layered on the side of the structure. Slight increases in the dimensions of wall thickness and step distance compared to the design specification were observed due to die swell. This is a normal phenomenon found when processing polymer melt from a small die orifice. Due to the same reason, the diameters of the holes were smaller than the design specification. Note that the structure was printed using 0.5mm layer thickness to minimise the melt residency time. Printing accuracy can be improved by using smaller layer thickness. Following this trial printing, different structures were designed and all had been successfully manufactured from PVOH using the pellet-fed material extrusion. The pellet-fed material extrusion demonstrated an excellent 3D printing capability to manufacture various structures in heat sensitive PVOH without a pre-processing step to produce thermoplastic filament.

Another advantage of pellet-fed material extrusion is to co-process and mix multiple materials with a controlled ratio during the process. This was demonstrated by co-processing PVOH with FWA and subsequently characterising the fluorescence effects of different segments of the printed samples. A strong UV-vis absorption peak between 300 nm and 450 nm was observed for all the segments from the sample containing 1 wt.% FWA additive (**Figure 8 a**), corresponding to the π- π^* transition in planar conjugated system [26]. Additionally, the fluorescence emission spectrum showed a strong peak at 439 nm for the PVOH sample with FWA additive (**Figure 8 b**). The light absorption in the UV region and re-emission at a higher wavelength demonstrated a fluorescence effect as a result of co-feeding FWA with PVOH into the printer. The fluorescence effect was observed by eye when the sample was exposed to UV light. This effect was exhibited on all fragments acquired from the printed sample. The absorption and emission peak intensity for different fragments was 1.35±0.08 and 190±10, respectively. The peak intensity was quantitatively affected by the amount of FWA in each fragment [22]. Small deviation of the data demonstrated homogeneous mixing of multiple materials during the printing process. Therefore, an additional process to pre-mix compounds was therefore unnecessary. The PVOH sample without FWA did not show the same peaks on either the absorption or emission spectra (**Figures 8a and 8b**).

The SEM images demonstrated a good inter-filament coalescence due to a deep penetration of polymer melt into the interface (**Figure 9**). The interface thickness and strength was determined by the extent of molecular chain penetration and the subsequent re-entanglement. However, one of the main drawbacks of hot-melt material extrusion AM is that structures are mechanically weak in the interfaces (1) between layers and (2) between neighbouring filaments within a layer due to the layer-by-layer printing pattern. Therefore, a deep interface penetration demonstrated in this study was beneficial to improve the overall quality of the printed structure. Further improvement in interlayered coalescence may be achieved by using a higher liquefier temperature or a lower molecular weight PVOH [27]. However, it is beyond the scope of this study.

3.3. Effects of Residency Time on PVOH

The material processed using pellet-fed material extrusion can have different residency time via feeding through different ports (or through using a different extrusion motor rpm to obtain different layer thicknesses). The decrease in peak intensity of the infrared band at 3450 cm^{-1} (O-H) demonstrated a more significant thermal decomposition of PVOH when the residency time increased from 14 min to 25 min (**Figure 10**). This confirms that the elimination of the hydroxyl group was affected by the duration of PVOH thermal exposure. The loss in the intensity of the O-H infrared peak has been reported to follow a first order rate in response to the residency time [9].

Thermal decomposition also resulted in significant ($p<0.05$) decrease in tensile properties when the residency time increased from 14 min to 25 min (**Figure 11**). It is postulated that the elimination of pendant groups reduced the rigidity of molecular chains, allowing disentanglement to occur more easily under external forces. Additionally, there was no significant difference ($p>0.05$) in the strain at break, indicating no breakdown in the backbone chain for samples heated under 25 min residency time. No distinct necking was observed from the tensile curves indicating the decrease in the cross-sectional area of PVOH samples was not by a greater proportion than the material strain hardened.

Due to the presence of the hydroxyl pendant group, most PVOH grades are soluble in water via the hydrogen bond formation between polymer and water molecules. Therefore, excessive elimination of the hydroxyl group may result in a loss in water solubility. PVOH processed under short residency time started to disintegrate from 4 min of immersion in the water bath, slightly earlier than the sample processed under long residency time (approx. 6 min). Nevertheless, both samples dissolved completely before 9 min of immersion, demonstrating good water solubility (**Figure 12**).

There may be a lack of direct comparison between this one-step melt process and the multi-step melt process as the material was not processed using traditional extrusion-based 3D printing. Notwithstanding this limitation, this study has showed the benefits of using a one-step melt process to manufacture PVOH, ensuring minimum loss in its mechanical properties and water solubility. The pellet-fed material extrusion combines compounding, filament extrusion, and 3D printing, and therefore, is an ideal AM technique to manufacture PVOH components. Multi-material printing with controlled feeding rates allows precise incorporation of laundry, agricultural, pharmaceutical, or medical active ingredients into PVOH with a pre-designed structure. The outcome of this study contributes to the continuous development of AM demonstrating a robust technique to improve the functionality of formulations and increase their potential applications.

4. Conclusion

This study has proposed to use a pellet-fed material extrusion technique to process heat-sensitive materials. This technique successfully requires only one melt processing techniques and therefore elegantly solves several major limitations of the current hot-melt AM techniques, such as found in traditional material extrusion. A great variety and combination of materials can be processed using this technique, creating more application opportunities using AM as the manufacturing tool. Multi-material printing was demonstrated by feeding PVOH with an additive at different rates and building a structure with composition homogeneously distributed. PVOH materials used in this study demonstrated T_m of 178°C, thermal decomposition temperature over 225°C, and a significant reduction in viscosity from 200°C. Based on the thermal properties, the extrusion and liquefier temperatures were set at 178°C and 200°C, respectively. The pellet-fed material extrusion allowed PVOH to be processed with reduced exposure to heat and therefore retain most of its functionality. Young's modulus, stress at 2 % strain, and stress at break increased significantly when PVOH was subjected to a short residency time (14 min) compared to a long residency time (25 min). Additionally, this technique demonstrated good 3D printing capability allowing formulations to be fabricated to well-designed structures with highly complex functionality to meet with the requirements of various applications. Potential future work is recommended to investigate the capability of using the screw-based extrusion to construct 3D geometries with a variable and controllable composition, which has always been a major limitation of extrusion-based 3D printing.

5. Acknowledgements

The authors acknowledge funding by Innovate UK under research project grant (101491) entitled 'PVOH Composite Active Packaging'.

References

[1] Hassan, C. and Peppas, N., 2000. Structure and applications of poly (vinyl alcohol) hydrogels produced by conventional crosslinking or by freezing/thawing methods. *Biopolymers· PVA Hydrogels, Anionic Polymerisation Nanocomposites*, pp.37-65.

[2] Finley, J.H., 1961. Spectrophotometric determination of polyvinyl alcohol in paper coatings. *Analytical Chemistry*, *33*(13), pp.1925-1927.

[3] Russo, M.A., O'Sullivan, C., Rounsefell, B., Halley, P.J., Truss, R. and Clarke, W.P., 2009. The anaerobic degradability of thermoplastic starch: polyvinyl alcohol blends: potential biodegradable food packaging materials. *Bioresource technology*, *100*(5), pp.1705-1710.

[4] Baker, M.I., Walsh, S.P., Schwartz, Z. and Boyan, B.D., 2012. A review of polyvinyl alcohol and its uses in cartilage and orthopedic applications. *Journal of Biomedical Materials Research Part B: Applied Biomaterials*, *100*(5), pp.1451-1457.

[5] Li, X., Kanjwal, M.A., Lin, L. and Chronakis, I.S., 2013. Electrospun polyvinyl-alcohol nanofibers as oral fast-dissolving delivery system of caffeine and riboflavin. *Colloids and Surfaces B: Biointerfaces*, *103*, pp.182-188.

[6] Goodship, V. and Jacobs, D.K., 2009. *Polyvinyl alcohol: materials, processing and applications* (Vol. 16, No. 12). Smithers Rapra Technology.

[7] Dong, W., Wang, Y., Huang, C., Xiang, S., Ma, P., Ni, Z. and Chen, M., 2014. Enhanced thermal stability of poly (vinyl alcohol) in presence of melanin. *Journal of Thermal Analysis and Calorimetry*, *115*(2), pp.1661-1668.

[8] Ballistreri, A., Foti, S., Montaudo, G. and Scamporrino, E., 1980. Evolution of aromatic compounds in the thermal decomposition of vinyl polymers. *Journal of Polymer Science Part A: Polymer Chemistry*, *18*(4), pp.1147-1153.

[9] Holland, B.J. and Hay, J.N., 2001. The thermal degradation of poly (vinyl alcohol). *Polymer*, *42*(16), pp.6775-6783.

[10] Shanjani, Y., Croos, D., Amritha, J.N., Pilliar, R.M., Kandel, R.A. and Toyserkani, E., 2010. Solid freeform fabrication and characterization of porous calcium polyphosphate structures for tissue engineering purposes. *Journal of Biomedical Materials Research Part B: Applied Biomaterials*, *93*(2), pp.510-519.

[11] Cox, S.C., Thornby, J.A., Gibbons, G.J., Williams, M.A. and Mallick, K.K., 2015. 3D printing of porous hydroxyapatite scaffolds intended for use in bone tissue engineering applications. *Materials Science and Engineering: C*, *47*, pp.237-247.

[12] Zhou, Z.X., Buchanan, F., Lennon, A. and Dunne, N., 2015. Investigating approaches for three-dimensional printing of hydroxyapatite scaffolds for bone regeneration. *Key Eng. Mater*, *631*, pp.306-311.

[13] Jeffries, E.M., Nakamura, S., Lee, K.W., Clampffer, J., Ijima, H. and Wang, Y., 2014. Micropatterning electrospun scaffolds to create intrinsic vascular networks. *Macromolecular bioscience*, *14*(11), pp.1514-1520.

[14] Salaoru, I., Zhou, Z., Morris, P. and Gibbons, G.J., 2016. Inkjet printing of polyvinyl alcohol multilayers for additive manufacturing applications. *Journal of Applied Polymer Science*, *133*(25).

[15] Salaoru, I., Zhou, Z., Morris, P. and Gibbons, G.J., 2017. Inkjet-printed polyvinyl alcohol multilayers. *JoVE (Journal of Visualized Experiments)*, (123), pp.e55093-e55093.

[16] Goyanes, A., Buanz, A.B., Basit, A.W. and Gaisford, S., 2014. Fused-filament 3D printing (3DP) for fabrication of tablets. *International journal of pharmaceutics*, *476*(1), pp.88-92.

[17] Skowyra, J., Pietrzak, K. and Alhnan, M.A., 2015. Fabrication of extended-release patient-tailored prednisolone tablets via fused deposition modelling (FDM) 3D printing. *European Journal of Pharmaceutical Sciences*, *68*, pp.11-17.

[18] Ni, F., Wang, G. and Zhao, H., 2017. Fabrication of water-soluble poly (vinyl alcohol)-based composites with improved thermal behavior for potential three-dimensional printing application. *Journal of Applied Polymer Science*, *134*(24).

[19] Tagami, T., Fukushige, K., Ogawa, E., Hayashi, N. and Ozeki, T., 2017. 3D Printing Factors Important for the Fabrication of Polyvinylalcohol Filament-Based Tablets. *Biological and Pharmaceutical Bulletin*, 40(3), pp.357-364.

[20] Zhou, Z., Salaoru, I., Morris, P. and Gibbons, G.J., 2016. Development of a Direct Feed Fused Deposition Modelling Technology for Multi-Material Manufacturing. *AIP Conference Proceedings*, 1769(1), pp.190004.

[21] Grimm, T.A., 2010. 3D Printer Benchmark North American Edition. *TA Grimm & Associates Inc*.

[22] Eng, L.K. and Cole, A.L.J., 1976. Tinopal AN in Fluorescent Microscopic Detection of Bacteria within Plant Tissues. *Stain Technology*, 51, pp. 277-278.

[23] Tsuchiya, Y. and Sumi, K., 1969. Thermal decomposition products of poly (vinyl alcohol). *Journal of Polymer Science Part A: Polymer Chemistry*, *7*(11), pp.3151-3158.

[24] Tubbs, R.K., 1965. Melting point and heat of fusion of poly (vinyl alcohol). *Journal of Polymer Science Part A: Polymer Chemistry*, *3*(12), pp.4181-4189.

[25] Venkataraman, N., Rangarajan, S., Matthewson, M.J., Harper, B., Safari, A., Danforth, S.C., Wu, G., Langrana, N., Guceri, S. and Yardimci, A., 2000. Feedstock material property-process relationships in fused deposition of ceramics (FDC). *Rapid Prototyping Journal*, 6, pp. 244-252.

[26] Yamaki, S.B., Barros, D.S., Garcia, C.M., Socoloski, P., Oliveira, O.N. and Atvars, T.D., 2005. Spectroscopic studies of the intermolecular interactions of Congo red and tinopal CBS with modified cellulose fibers. *Langmuir*, *21*(12), pp.5414-5420.

[27] McIlroy, C. and Olmsted, P.D., 2017. Deformation of an amorphous polymer during the fused-filament-fabrication method for additive manufacturing. *Journal of Rheology*, *61*(2), pp.379-397.

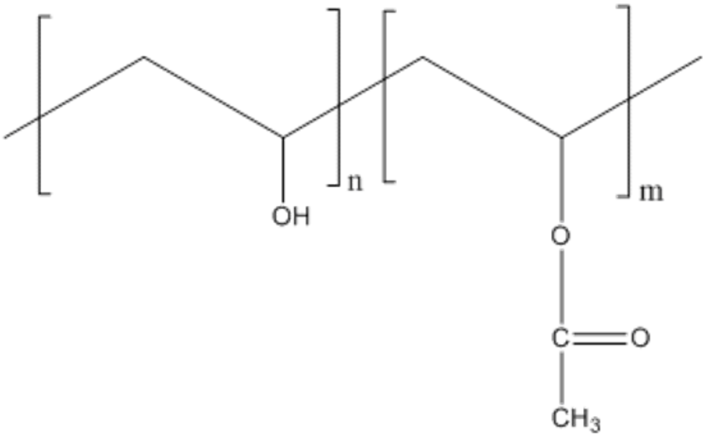

Hydrolysis level (mol.%): n/(n+m) x 100%

Figure 1: Structure of patially hydrolysed PVOH.

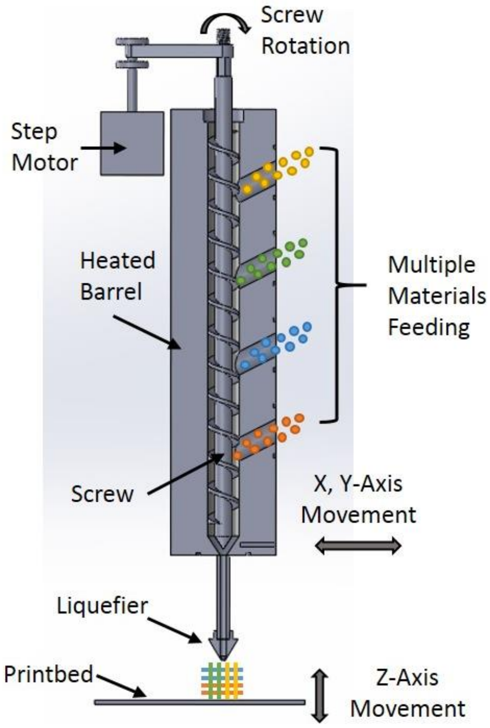

Figure 2: Schematic of the pellet-fed material extrusion system developed in this study. Barrel, liquefier and their connecting tube were displaced in section view to expose their interior construction.

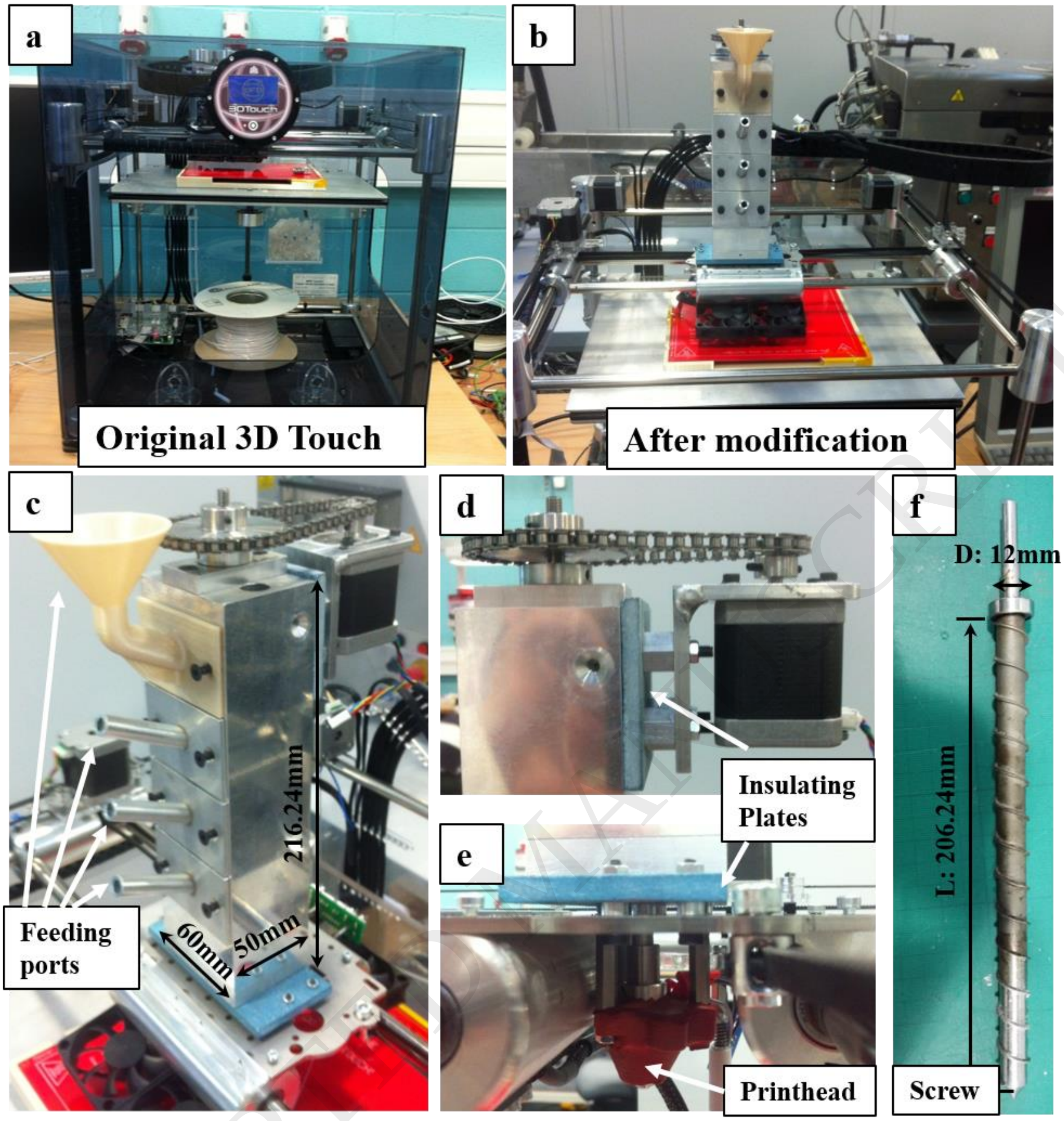

Figure 3: Modification of a FDM machine: (a) the original 3D Touch FDM machine; (b) pellet-fed material extrusion machine, modified from the 3D Touch; (c) the barrel and multiple feeding ports; (d) a stepper motor controlling the rotational speed of screw; (e) the printhead connected to the extruder; and (f) the single screw.

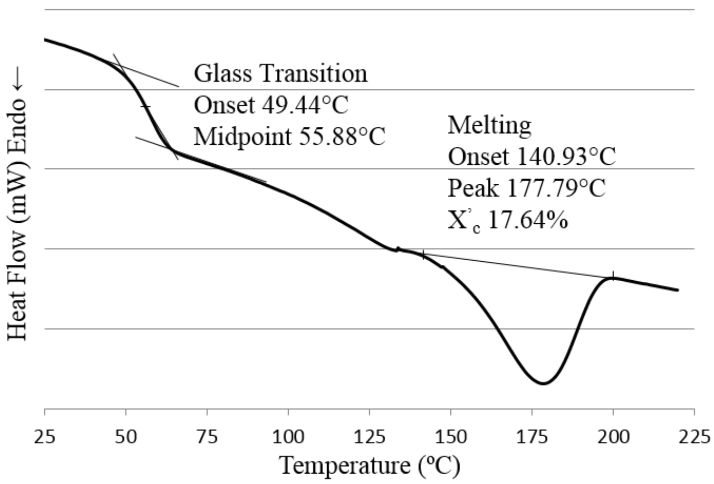

Figure 4: DSC thermogram for a heating curve of PVOH in nitrogen atmosphere from 25°C to 225°C at a heating rate of 10°C/min.

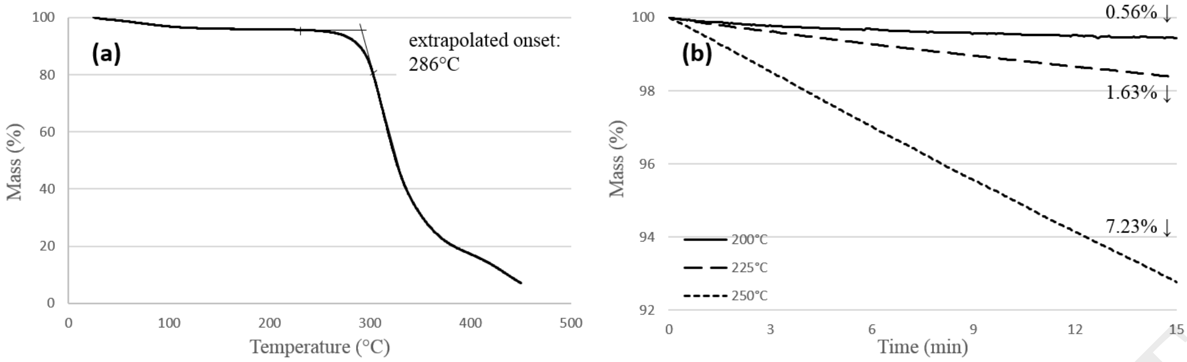

Figure 5: TGA curves for PVOH in nitrogen atmosphere under dynamic and isothermal conditions: (**a**) from 25°C to 450°C at a heating rate of 10°C/min; and (**b**) 15min heating at 200, 225, and 250°C.

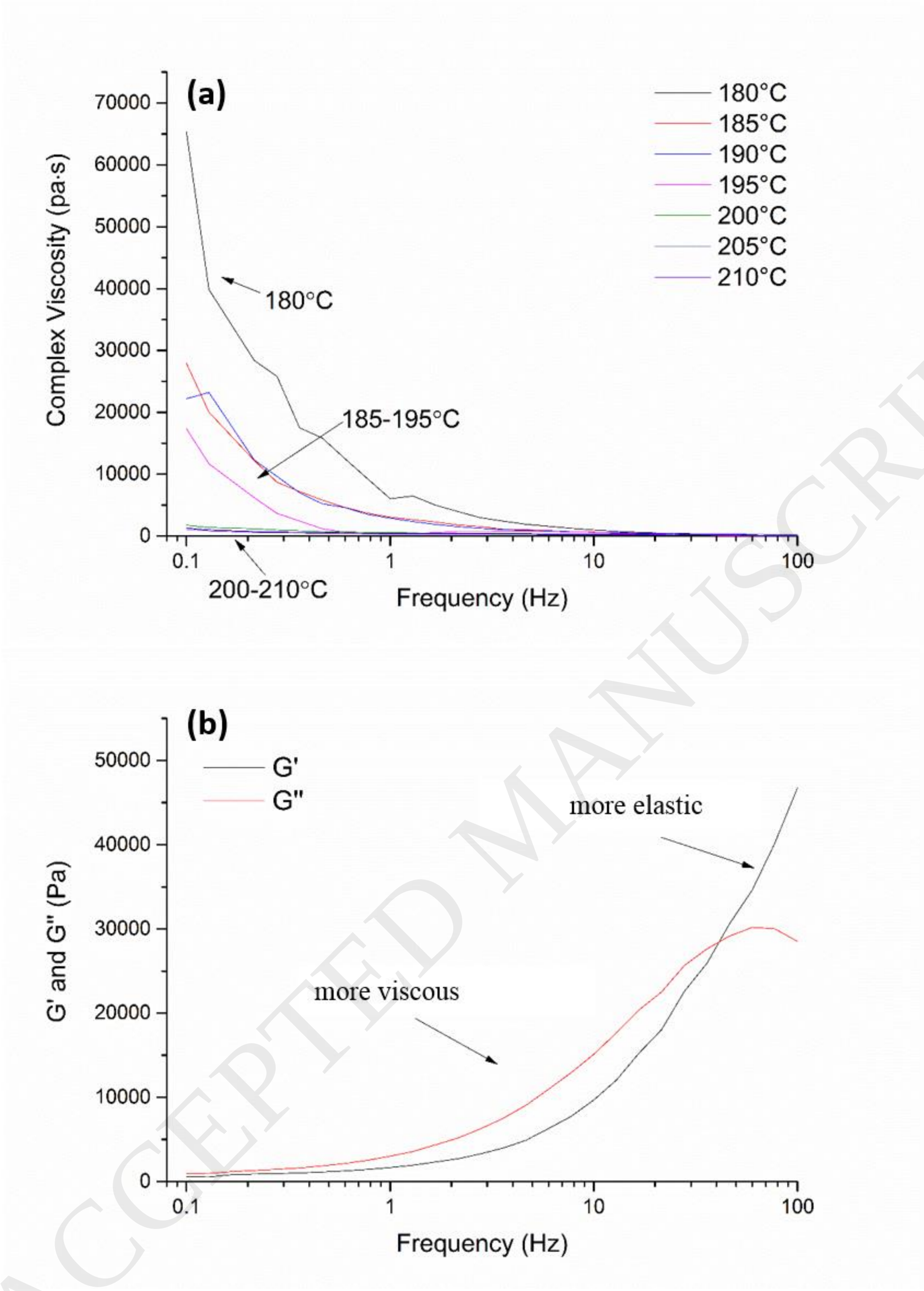

Figure 6: Oscillatory rheology for PVOH: (a) plots of complex viscosity versus log frequency at different temperatures; and (b) plots of storage modulus (G') and loss modulus (G'') versus log frequency at 200°C.

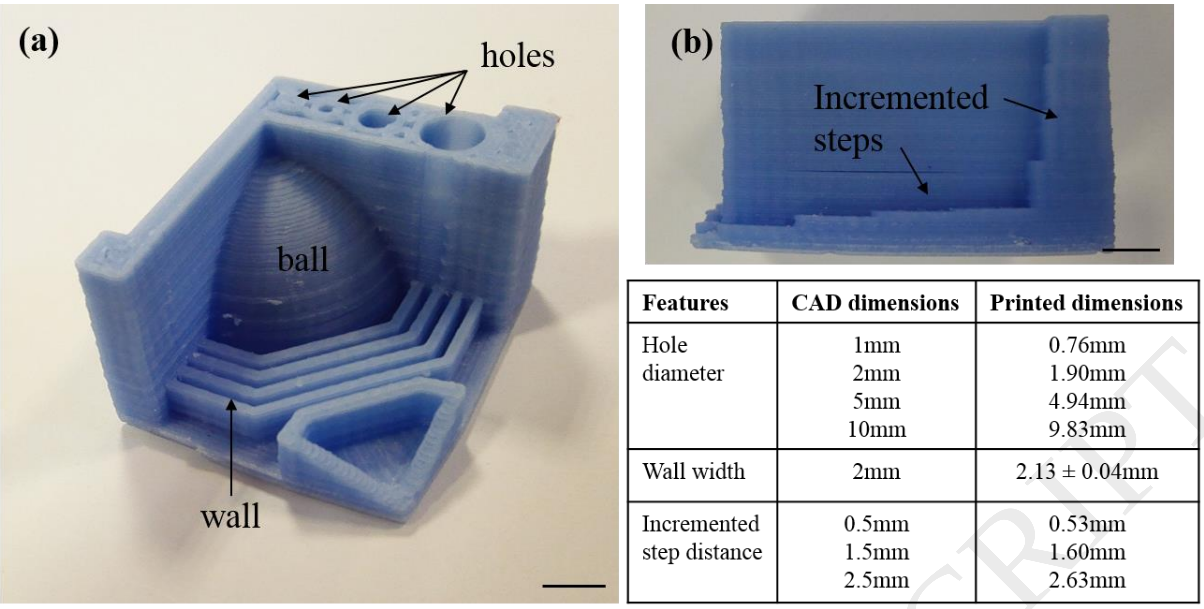

Features	CAD dimensions	Printed dimensions
Hole diameter	1mm 2mm 5mm 10mm	0.76mm 1.90mm 4.94mm 9.83mm
Wall width	2mm	2.13 ± 0.04mm
Incremented step distance	0.5mm 1.5mm 2.5mm	0.53mm 1.60mm 2.63mm

Figure 7. (**a**) Front and (**b**) side views of a printed PVOH structure comprising different features to demonstrate the 3D printability of the direct-feed FDM. Scale bar = 10mm.

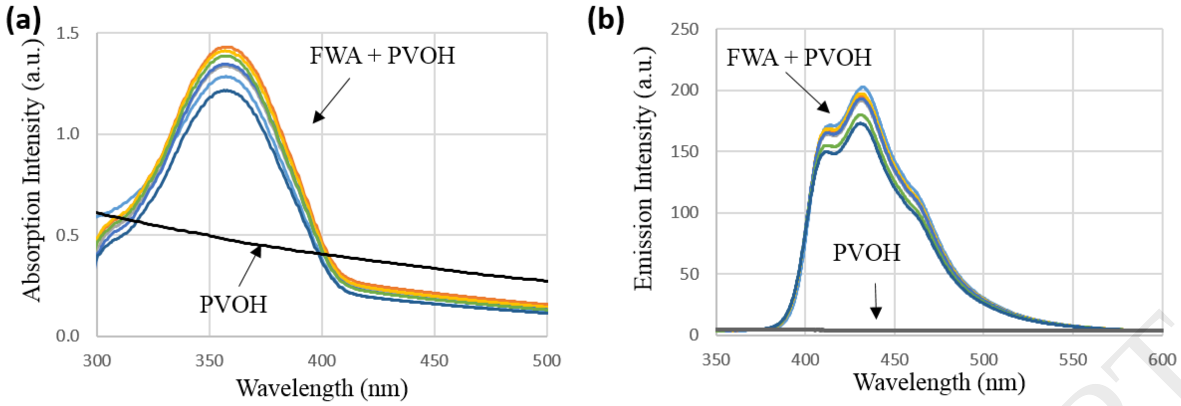

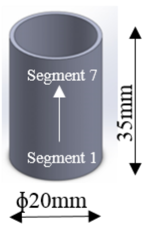

	Segments on a FWA+PVOH structure									PVOH
	1	2	3	4	5	6	7	Mean	SD	
Absorption Peak Intensity (a.u.)	1.29	1.43	1.34	1.41	1.35	1.39	1.22	1.35	0.08	0.52
Emission Peak Intensity (a.u.)	203	196	192	197	193	180	173	190	10	4.27

Figure 8: (**a**) UV-vis absorption spectra and (**b**) fluorescence emission spectra of different segments from the structure co-printed from PVOH and 1wt.% FWA. Spectra of PVOH without addition of FWA are also presented. The absorption and emission peak intensity for different segments of a structure containing FWA and PVOH was listed with mean±SD, compared with that for a structure containing only PVOH.

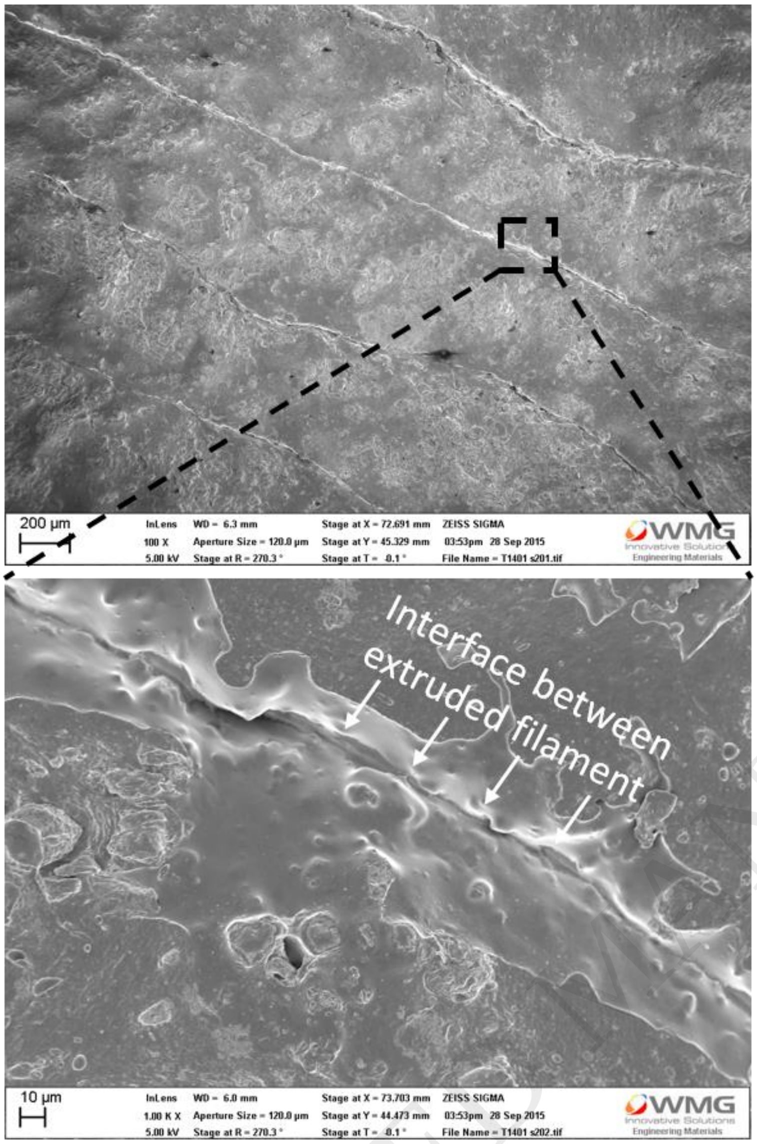

Figure 9: SEM images of PVOH surface manufactured using pellet-feed material extrusion at low magnification of x100 and magnified view of the black rectangular (x1000).

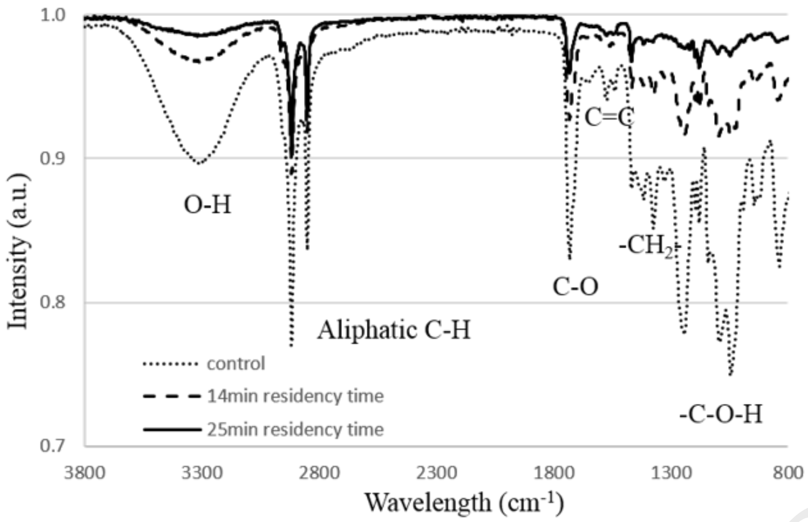

Figure 10: FTIR spectrum of PVOH subjected to residency times of 14 minutes and 25 minutes under the AM process of pellet-feed material extrusion, compared to the control sample (0 residency time).

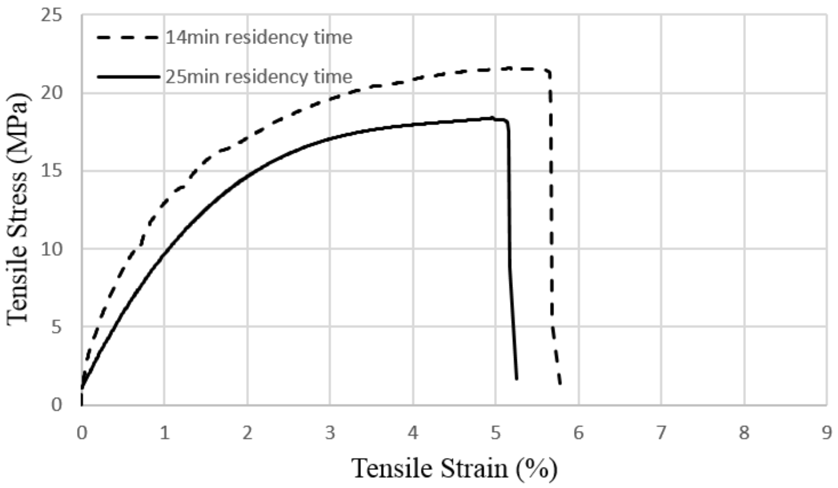

	Value at 14 min residency time (mean±SD)	Value at 25 min residency time (mean±SD)	Decrease in mean value (%)
Young’s modulus	1.8±0.2 GPa ***	0.9±0.2 GPa	49
Stress at 2% strain	18±1 MPa **	13±3MPa	29
Stress at break	21.3±0.3 MPa **	18±3 MPa	16
Strain at break	5±1 %	6±2 %	-17

Figure 11: Tensile properties of the PVOH (mean ± SD) and difference in mean values (%) when subjected to residency times of 14 minutes and 25 minutes. ** $p<0.05$ and *** $p<0.001$, indicating a significant difference between 14min and 25min residency time. The stress-vs.-strain curves of one sample from each residency time were plotted as examples.

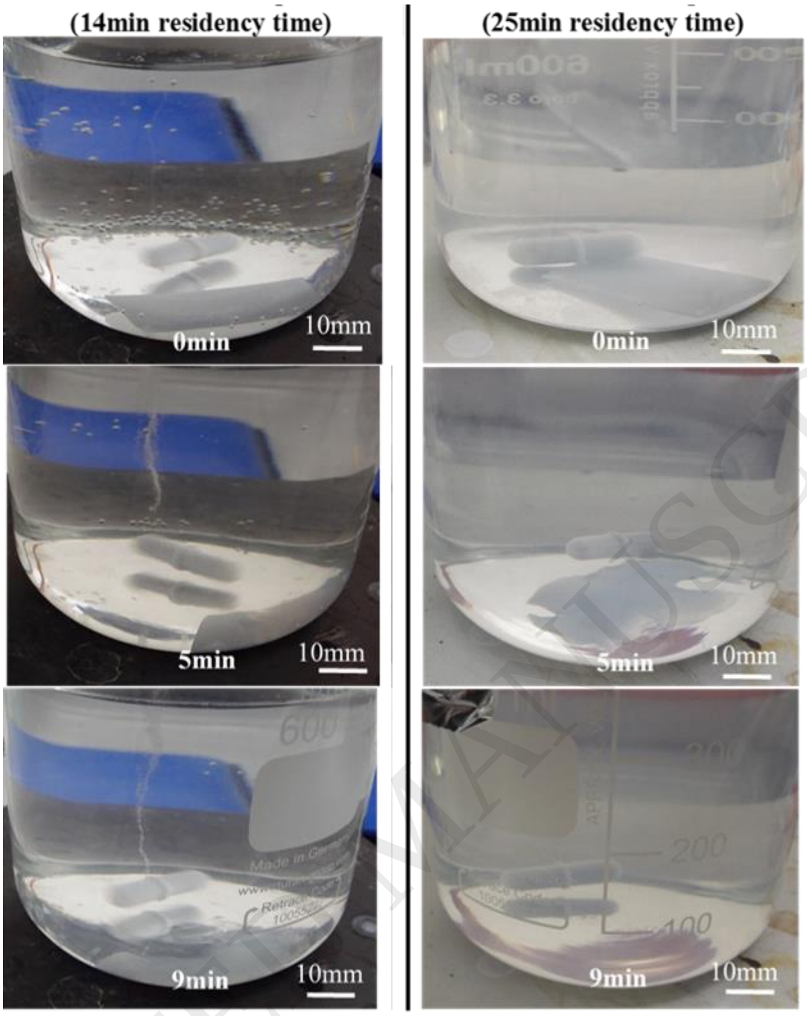

Figure 12: Water solubility tests of PVOH subjected to residency times of 14 minutes and 25 minutes under the AM process of pellet-feed material extrusion.